

# On the initiation of wedge-type cracks at grain-boundary triple junctions during high-temperature creep

MANABU TANAKA, HIROSHI IIZUKA

*Department of Mechanical Engineering for Production, Mining College of Akita University, Akita 010, Japan*

The typical grain boundary cracks are often formed at the grain-boundary triple junction as a result of blocking of grain-boundary sliding. However, a theoretical discussion has not fully been made on the nucleation of grain corner cracks at high temperatures where diffusional recovery occurs. In this study, a continuum mechanics model which incorporated the recovery effect by diffusion of atoms has been developed to explain the initiation of wedge-type cracking during high-temperature creep. A good agreement was found between the result of calculation based on this model and experimental results in austenite steels. It was considered that there is a critical creep rate for wedge-type cracking. The model was also applied to the prediction of the rupture life in creep.

## 1. Introduction

It is well known that there are two types of intergranular creep cracks, namely, wedge-type cracks and round-type cavities, and that they are formed as a result of grain-boundary sliding [1]. The typical grain-boundary cracks are often nucleated at the grain-boundary triple junction where high stress concentration is caused by blocking of grain-boundary sliding, while round-type cavities are usually associated with irregularities [2] or second-phase particles [3] on the grain boundary. The diffusion of atoms at elevated temperatures as well as plastic accommodation results in a decrease of the stress concentration at the grain corner or at the interface of second-phase particles. Mori *et al.* [4] recently discussed the blocking of grain-boundary sliding by second-phase particles, using a continuum mechanics model which incorporated the recovery effect by diffusion of atoms. However, the theoretical analysis has not been made on the nucleation of grain corner cracks at high temperatures where diffusional recovery occurs.

In this study, a continuum mechanics model which is similar to that of the previous study [5] has been developed to explain the crack initiation at the grain-boundary triple junction during

high-temperature creep. It is also important to know the crack initiation life for life prediction in the material in which the creep rupture occurs immediately after the crack initiation [6]. The model was applied to the prediction of rupture life. The result of theoretical calculation was then compared with that of experiment in austenite steels.

## 2. Elastic strain energy and internal stress arising from blocking of grain-boundary sliding

The internal stress state when grain-boundary sliding is blocked at the grain corner can be calculated by Eshelby's method [7], if a grain-boundary is approximated to be a flat ellipsoidal inclusion [8]. A grain-boundary is assumed here to be a two-dimensional flat inclusion,  $D_0$ , with length  $2a_1$  and thickness  $2a_2$ .

$$x_1^2/a_1^2 + x_2^2/a_2^2 \leq 1 \quad (a_2/a_1 \ll 1) \quad (1)$$

As shown in Fig. 1a,  $2a_1$  and  $2a_2$  are assumed to be equal to the grain-boundary length,  $2L$ , and the magnitude of Burgers vector,  $b$ , respectively.

We consider that plastic shear strain on the grain-boundary,  $\gamma_{21}^* = 2\epsilon_{21}^*$  ( $= 2\epsilon^*$ ) occurs as a

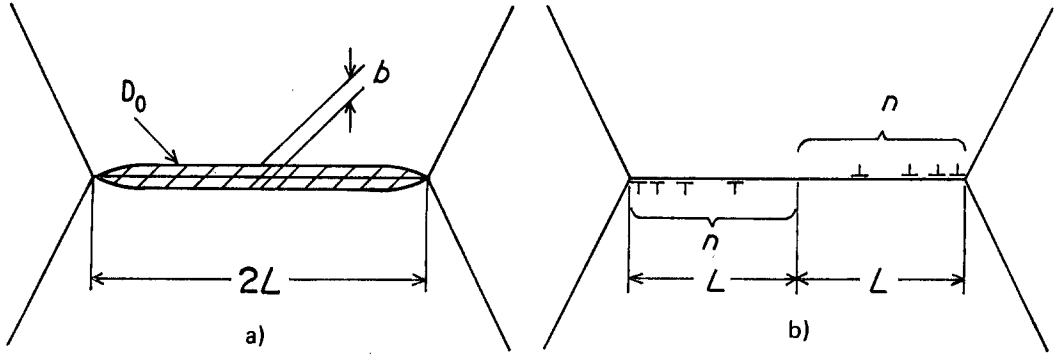


Figure 1 Grain boundary approximated by a two-dimensional flat inclusion,  $D_0$ .

result of grain-boundary sliding under an external tensile stress,  $\sigma^A$ . If the sliding is blocked at the grain corner, eigen strain  $-\epsilon_{21}^*$  ( $= -\epsilon^*$ ) occurs in the domain  $D_0$  which is otherwise free sliding. The internal stress in the inclusion,  $\tau_{in}$ , is given by [9]

$$\tau_{in} = -2A \left( \frac{b}{2L} \right) \mu \epsilon_{21}^* = -2A \left( \frac{b}{2L} \right) \mu \epsilon^* \quad (2)$$

where  $\mu$  and  $\nu$  are the rigidity and Poisson's ratio of the material, respectively, and  $A = 1/(1 - \nu)$ . The elastic strain energy arising from blocking of grain-boundary sliding,  $E_{el}$ , is

$$E_{el} = 2A \left( \frac{b}{2L} \right) \mu \epsilon_{21}^{*2} V = 2A \left( \frac{b}{2L} \right) \mu \epsilon^{*2} V \quad (3)$$

where the volume of the inclusion,  $V$ , is  $\pi Lb/2$  per unit width of the material. The shear strain,  $\epsilon_{21}^*$ , on the grain boundary can be replaced by the conjugate slip of  $n$  dislocations with the same Burgers vector,  $b$ , on a half of the grain-boundary length,  $L$  (Fig. 1b) (or the slip of a pair of dislocations with Burgers vector  $nb$ ). As the total displacement of dislocations is  $nb$  on the grain-boundary length,  $2L$ , the local strain,  $\epsilon^*$ , is defined by

$$\epsilon^* = \frac{nb/2}{b} = \frac{n}{2} \quad (4)$$

Substituting Equation 4 into Equation 3,  $E_{el}$  can be rewritten as follows:

$$E_{el} = 2A \left( \frac{b}{2L} \right) \left( \frac{n}{2} \right)^2 \mu \frac{\pi Lb}{2} = \frac{\pi A \mu n^2 b^2}{8} \quad (5)$$

### 3. Internal stress and eigen strain in inclusion $D_0$

The total number of atoms contained in extra half planes of  $n$  dislocations with unit width,  $N$ , is

expressed by the grain diameter,  $D$ , and the atomic volume of the material,  $\Omega$ :

$$N = \frac{nbD}{\Omega} = \frac{2\epsilon^* bD}{\Omega} \quad (6)$$

In the absence of recovery, the total number of atoms,  $N_0$ , is given by the corresponding plastic strain,  $\epsilon$ , and the number of dislocations,  $n_0$ :

$$N_0 = \frac{n_0 b D}{\Omega} = \frac{2\epsilon b D}{\Omega} \quad (7)$$

Fig. 2 shows the deficit and excess of mass caused as a result of blocking of the grain-bound-

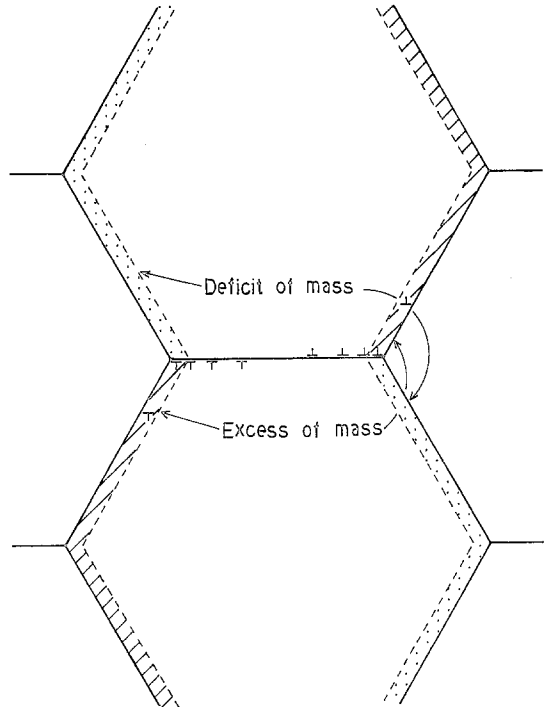


Figure 2 Deficit and excess of mass caused by blocking of the grain-boundary sliding.

ary sliding.  $N$  is also the net excess of atoms which should be transported. Emission of atoms,  $dN$ , from the side of excessive mass occurs when dislocations climb along the grain boundary in the recovery process. Those atoms are transported by diffusion along the grain boundary or through the grain to the deficit side of mass. The difference in chemical potential between the emission and the absorption sides of atoms,  $\mu^*$ , is given by [5]

$$\begin{aligned}\mu^* &= \frac{dE_{el}}{dN} = \frac{dn}{dN} \frac{dE_{el}}{dn} \\ &= \frac{\Omega}{bD} \frac{\pi A \mu n b^2}{4} = \frac{\pi A \mu n b \Omega}{4D}\end{aligned}\quad (8)$$

When the recovery is controlled by grain-boundary diffusion, the flux of atoms,  $J_{GB}$ , is expressed by the following equation, provided that the average migration distance of atoms is  $4L$ :

$$\begin{aligned}J_{GB} &= \frac{D_{GB}}{\Omega k T} \text{grad } \mu^* = \frac{D_{GB}}{\Omega k T} \frac{\pi A \mu n b \Omega / 4D}{4L} \\ &= \frac{\pi A \mu \Omega D_{GB} N}{16 L D^2 k T}\end{aligned}\quad (9)$$

where  $D_{GB}$  is the grain-boundary diffusion coefficient,  $k$  Boltzmann's constant and  $T$  the absolute temperature. The thickness of the cross-section of grain-boundary diffusion,  $\delta$ , is approximately equal to  $2b$ .

Since the emission of atoms occurs from a pair of the extra half planes, the total migration rate of atoms due to grain-boundary diffusion,  $(dN/dt)_{GB}$ , is given by

$$\begin{aligned}\left(\frac{dN}{dt}\right)_{GB} &\doteq 2\delta J_{GB} = \frac{\pi A \mu D_{GB} \Omega N \delta}{8 L D^2 k T} \\ &= \frac{\pi(3)^{1/2} A \mu D_{GB} \Omega N \delta}{4 D^3 k T}\end{aligned}\quad (10)$$

where  $L$  is approximated by  $D/2(3)^{1/2}$ . If the climb of grain-boundary dislocation is controlled by volume diffusion, the cross-section of diffusion is  $2D$  per unit width and the diffusion distance is approximated to be  $D$ . Therefore, the diffusion flux,  $J_v$ , is given by

$$\begin{aligned}J_v &= \frac{D_v}{\Omega k T} \text{grad } \mu^* = \frac{D_v}{\Omega k T} \frac{\pi A \mu n b \Omega / 4D}{D} \\ &= \frac{\pi A \mu D_v \Omega N}{4 D^3 k T}\end{aligned}\quad (11)$$

where  $D_v$  is the volume diffusion coefficient. The

migration rate,  $(dN/dt)_v$ , in this case is expressed by

$$\left(\frac{dN}{dt}\right)_v \doteq 2D J_v = \frac{\pi A \mu D_v \Omega N}{2 D^2 k T}\quad (12)$$

From Equations 10 and 12,

$$\frac{(dN/dt)_v}{(dN/dt)_{GB}} = \frac{2D_v D}{3^{1/2} D_{GB} \delta} < 1\quad (13)$$

if the grain-boundary diffusion controls the recovery process. For example, substituting  $4.56 \times 10^{-19} \text{ m}^2 \text{ sec}^{-1}$  [5] and  $3.24 \times 10^{-13} \text{ m}^2 \text{ sec}^{-1}$  [10] for  $D_v$  and  $D_{GB}$  of the steels at 973 K, respectively, Equation 13 is satisfied when  $D$  is less than  $3.13 \times 10^{-4} \text{ m}$ . Differentiating  $N$  and  $N_0$  in Equations 6 and 7 with respect to time,  $t$ , we obtain

$$\frac{dN}{dt} = \frac{2bD}{\Omega} \frac{d\epsilon^*}{dt}\quad (14)$$

$$\frac{dN_0}{dt} = \frac{2bD}{\Omega} \frac{d\epsilon}{dt}\quad (15)$$

In the recovery process controlled by grain-boundary diffusion, the net migration rate,  $dN/dt$ , is given by

$$\frac{dN}{dt} = \frac{dN_0}{dt} - \left(\frac{dN}{dt}\right)_{GB}\quad (16)$$

Substituting Equations 14 and 15 into Equation 16, and using Equation 10, the following equation of primary reaction is obtained:

$$\begin{aligned}\frac{d\epsilon^*}{dt} &= \frac{d\epsilon}{dt} - \frac{\pi(3)^{1/2} A \mu D_{GB} \Omega \delta}{4 D^3 k T} \epsilon^* \\ &= \dot{\epsilon} - C \epsilon^*\end{aligned}\quad (17)$$

where  $\dot{\epsilon} = d\epsilon/dt$  and  $C = \pi(3)^{1/2} A \mu D_{GB} \Omega \delta / 4 D^3 k T$ . If the above equation is solved under the initial condition of  $\epsilon^* = 0$  for  $t = 0$  when  $\dot{\epsilon}$  is constant,

$$\epsilon^* = \frac{\dot{\epsilon}}{C} [1 - \exp(-Ct)]\quad (18)$$

The internal stress,  $\tau_{in}$ , is then given by

$$\tau_{in} = -2A \left(\frac{b}{2L}\right) \mu \frac{\dot{\epsilon}}{C} [1 - \exp(-Ct)]\quad (19)$$

If the volume diffusion controls the recovery process, the value of  $C$  in the above equations should be replaced by  $\pi A \mu D_v \Omega / 2 D^2 k T$ .

The term of an external stress,  $\sigma^A$ , does not appear in the above equations, because there is no interaction between an external stress and the internal stress field as regards the elastic strain energy (Colonnetti's theorem) [11].

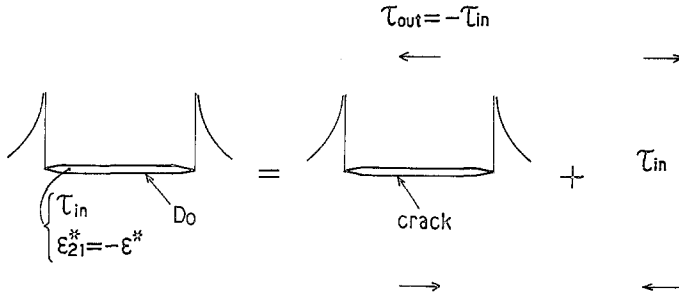


Figure 3 Stress field outside the inclusion  $D_0$ .

#### 4. Stress outside inclusion $D_0$ and critical strain rate for crack initiation

The stress field outside the flat inclusion  $D_0$  can be easily obtained by Mura's alternative method [12]. The internal stress in the domain  $D_0$ ,  $\tau_{in}$ , can be calculated by Equation 19. We consider an ellipsoidal notch which has the same shape and size as the inclusion  $D_0$ . This notch can be regarded as a crack, because the inclusion  $D_0$  is an extremely flat ellipsoid ( $b \ll 2L$ ) and  $\rho \cong 0$  ( $\rho$  is the radius of curvature at the notch root). According to the result of Stroh's calculation [13], the stress distribution around a crack in a body under a uniformly applied stress,  $\tau_{out}$ , can be also obtained without difficulty by putting  $\tau_{out} = -\tau_{in}$ . We next consider an infinite body without any cracks under a uniformly applied stress,  $\tau_{in}$ . The stress outside the flat inclusion  $D_0$  can be obtained by superposing Stroh's solution of a crack and a uniformly applied stress field,  $\tau_{in}$ , as shown in Fig. 3.

Stroh [13] also calculated the normal stress acting on the plane making an angle  $\theta$  with the slip plane. This stress is a maximum when  $\theta$  is  $70.5^\circ$ . The maximum value of the normal stress is  $(2/3^{1/2})(L/r)^{1/2} \tau_{out}$  at the distance  $r$  from the grain corner. For the initiation of intergranular wedge-type cracking, McLean [14] utilized Stroh's equation

$$\tau_{out} > \left[ \frac{12\gamma\mu}{\pi(1-\nu)L} \right]^{1/2} \quad (20)$$

where  $\gamma$  is the surface energy per unit area. The grain-boundary sliding in two directions, as shown in Fig. 4, is considered in this study. The wedge-type cracking can occur on the grain-boundary plane  $\overline{OA}$ . The normal stress acting on the plane  $\overline{OA}$  is  $2\tau_{out}$  in this case. Therefore, from Equation 2,

$$\begin{aligned} 2\tau_{out} &= -2\tau_{in} = \frac{4}{1-\nu} \left( \frac{b}{2L} \right) \mu \epsilon^* \\ &> \left[ \frac{12\gamma\mu}{\pi(1-\nu)L} \right]^{1/2} \end{aligned} \quad (21)$$

The critical shear strain for the crack initiation is given by

$$\epsilon^* > \frac{(1-\nu)L}{2b\mu} \left[ \frac{12\gamma\mu}{\pi(1-\nu)L} \right]^{1/2} = \left[ \frac{3\gamma(1-\nu)L}{\pi\mu b^2} \right]^{1/2} \quad (22)$$

The interaction between two sliding boundaries is neglected here. The critical strain rate,  $\dot{\epsilon}_c$ , necessary for wedge-type cracking at the time  $t_c$  is also given from Equation 18 by

$$\dot{\epsilon} > \dot{\epsilon}_c = \frac{C[3\gamma(1-\nu)L/\pi\mu b^2]^{1/2}}{1 - \exp(-Ct_c)} \quad (23)$$

The other type of intergranular cracking such as round-type cavity may occur below this critical strain rate. The effect of an external tensile stress,  $\sigma^A$ , on the crack initiation is negligible, because it is usually very small compared with the theoretical strength of the material ( $\cong E/10$ ).

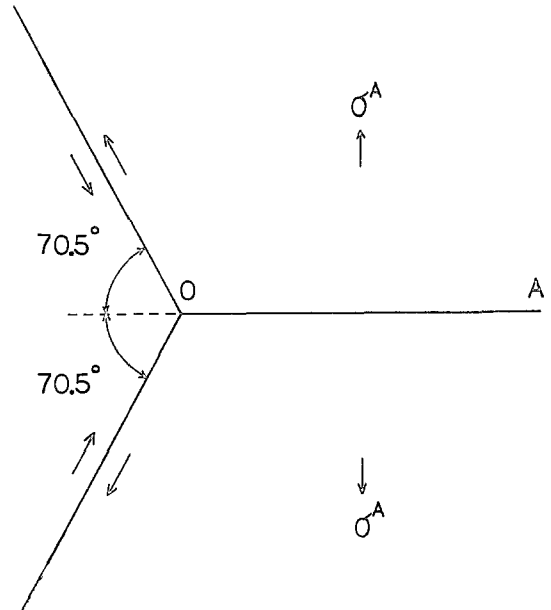


Figure 4 Grain-boundary sliding model considered in this study.

$\dot{\epsilon}_c$  can be connected with the steady-state creep rate,  $\dot{\epsilon}_s$ , which reflects materials properties when most of the rupture life is occupied by steady-state creep. If the recovery also involves another process such as plastic relaxation in the adjacent grains, the critical strain rate for wedge-type cracking is much larger than that calculated by Equation 23. Therefore, the calculated value,  $\dot{\epsilon}_c$ , gives the lower limit of the critical strain rate for wedge-type cracking. It is also known from Equation 23 that  $C[3\gamma(1-\nu)L/\pi\mu b^2]^{1/2}$  is the minimum value of  $\dot{\epsilon}_c$  at  $t_c = \infty$ .

### 5. Critical creep rate for initiation of wedge-type cracking and life prediction

We consider that the pure grain-boundary sliding occurs in the inclusion  $D_0$  with thickness  $b$ , while most of the creep deformation occurs within the grain. It is assumed in the calculation that the shear strain rate on the grain boundary,  $\dot{\epsilon}_g$ , is given by the following equation, although the experimental result is not generally obtained on the amount of the pure grain-boundary sliding:

$$\dot{\epsilon}_g = \frac{D}{b} \frac{3}{2} \lambda K \dot{\epsilon}_s \quad (24)$$

where  $\dot{\epsilon}_s$  is the steady-state creep rate and  $\lambda$  is the ratio of the shear strain rate on the grain boundary to the total creep rate.  $K$  is a direction coefficient,  $\sin \varphi \cos \varphi$ , where  $\varphi$  is the angle between sliding direction and tensile axis, and is  $70.5^\circ$  in this case. It is also assumed that  $\lambda$  is almost the same as the ratio of the grain-boundary strain to the total creep strain and is in the range from 0.02 to 0.1 under the usual creep stresses in stainless steels [15]. For  $\dot{\epsilon}_g = \dot{\epsilon}_c$ , the critical creep rate for the initiation of wedge-type cracking is given by

$$\dot{\epsilon}_s > \dot{\epsilon}_{sc} = \frac{2b}{3D\lambda K} \dot{\epsilon}_c \quad (25)$$

The value of  $\dot{\epsilon}_{sc}$  calculated by Equation 25 gives the lower limit of creep rate for crack initiation in connection with Equation 23.

Fig. 5 shows an example of wedge-type cracking observed in an austenitic 21Cr–4Ni–9Mn steel [5, 6]. Fig. 6 shows the result of calculation by Equation 25 in comparison with that of creep rupture test on austenite steels. In this calculation, the wedge-type cracking is assumed to occur at 80% of the rupture life. It was considered in those steels that the grain-boundary diffusion of atoms controls the recovery process, because Equation

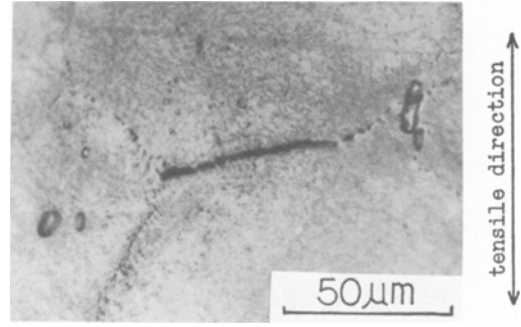


Figure 5 Typical wedge-type crack on grain-boundary in austenitic 21Cr–4Ni–9Mn steel ( $\sigma^A = 196$  MPa,  $T = 973$  K).

13 is satisfied in this case.  $b$  is  $2.55 \times 10^{-10}$  m for austenite steels and  $2\gamma$  is  $(2\gamma_s - \gamma_{GB})$ , where  $\gamma_s$  ( $1.95 \text{ J m}^{-2}$ ) and  $\gamma_{GB}$  ( $0.70 \text{ J m}^{-2}$ ) are the surface energy and the grain-boundary energy of  $\gamma$ -Fe [16], respectively. The other numerical values of physical constants used in the calculation are  $D_{GB} = 3.24 \times 10^{-13} \text{ m}^2 \text{ sec}^{-1}$  (973 K) [10],  $\Omega = 7.101 \times 10^{-5} \text{ m}^3 \text{ mol}^{-1}$  [5],  $\mu = 5.586 \times 10^4 \text{ MPa}$  [17] and  $\nu = 0.29$  [17]. A good agreement was found between the calculated steady-state creep rate and the experimental value in those steels, in spite of the rough estimation of the amount of grain-boundary sliding in the calculation. It is considered from this figure that the wedge-type cracking cannot be observed below a certain critical creep rate. Fig. 7 shows the effect of grain size on the critical creep rate for wedge-type cracking at 80% of the rupture life and the steady-state creep rate in an austenitic heat-resisting steel. For simplicity, the calculation was made only on the recovery by volume diffusion of atoms. It is found that the wedge-type crack is apt to be formed in the steel with the larger grain size under the same creep condition. Both the wedge-type crack and the round-type cavity can be sometimes observed in the same specimen, because there is a variation in the amount of grain-boundary sliding.

The rupture life can be predicted by Equations 23 and 25, when most of it is spent for the initiation of the wedge-type cracking [6]. Putting  $K = \sin 70.5^\circ \cos 70.5^\circ = 2(2)^{1/2}/9$ , the rupture life,  $t_c$ , is expressed by the following equation:

$$t_c = -\frac{1}{C} \ln \left\{ 1 - \frac{C}{\lambda \dot{\epsilon}_s} \left[ \frac{9\gamma(1-\nu)}{8\pi\mu L} \right]^{1/2} \right\} \quad (26)$$

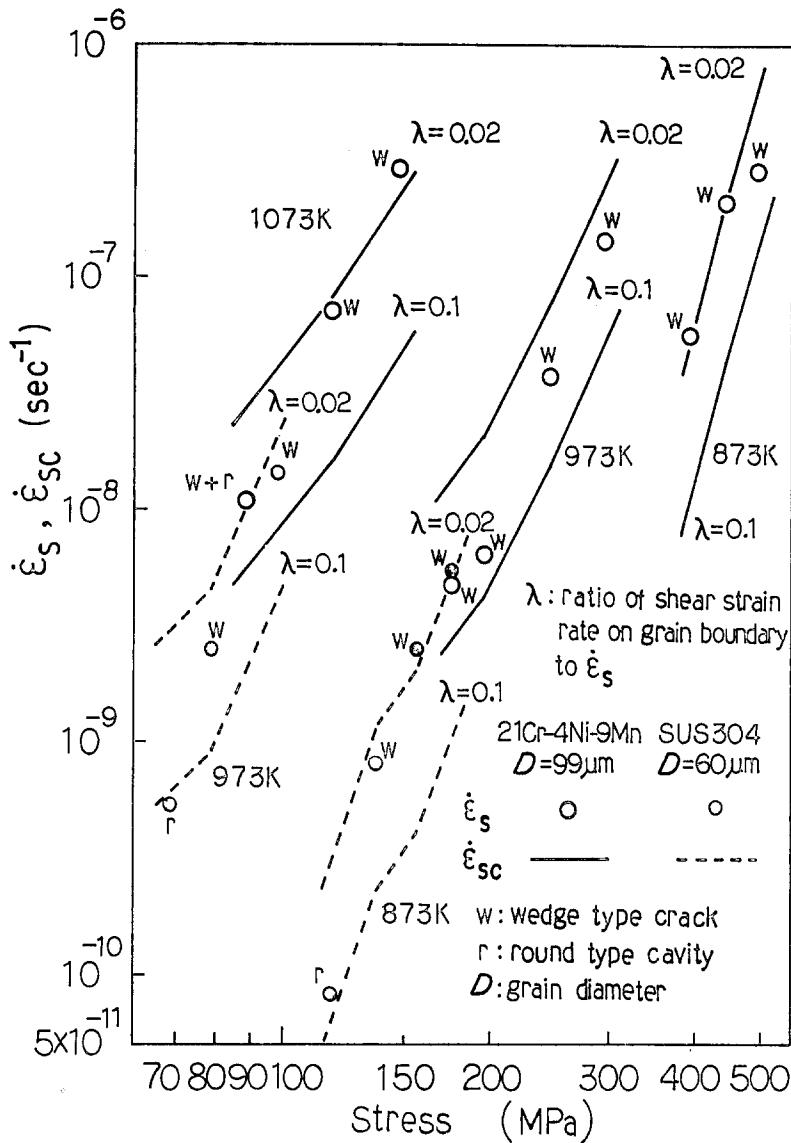


Figure 6 Critical creep rate for wedge-type cracking,  $\dot{\epsilon}_{sc}$ , and steady-state creep rate,  $\dot{\epsilon}_s$ , in austenite steels.

Fig. 8 shows the rupture life estimated by Equation 26 and that of the experiment in austenite steels in the creep range where wedge-type cracking occurs [6, 19]. Most of the data points lie between two calculated values for  $\lambda$  in 21Cr-4Ni-9Mn steel, while the calculated rupture life is somewhat shorter than the experimental life under stresses at 873 K in SUS304 steel. This may be due to the effect of the other recovery process such as plastic accommodation in the adjacent grains, or to the fact that the wedge-type cracking in SUS304 steel can occur in the relatively early stage of creep at low stress level [18].

The continuum mechanics model used in this study can be also applicable to the understanding

of crack initiation when the strain rate changes periodically or with time in fatigue. The study is now in progress.

## 6. Conclusion

A theoretical discussion was made on the initiation of the intergranular wedge-type crack in creep, using a continuum mechanics model which incorporated the recovery effect by diffusion of atoms. A good agreement was found between the result of calculation based on this model and that of experiment in austenite steels. It was considered that there is a critical creep rate for wedge-type cracking. The result of calculation gives the lower limit of a critical creep rate for crack initiation,

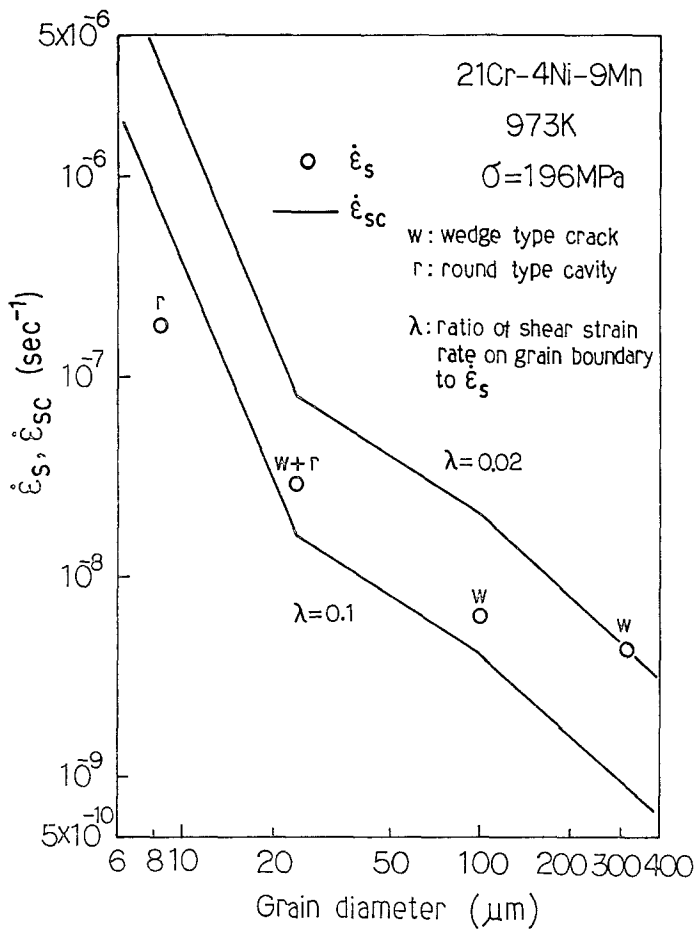


Figure 7 Grain size dependence of critical creep rate for wedge-type cracking,  $\dot{\epsilon}_{sc}$ , and steady-state creep rate,  $\dot{\epsilon}_s$ , in austenitic 21Cr-4Ni-9Mn steel.

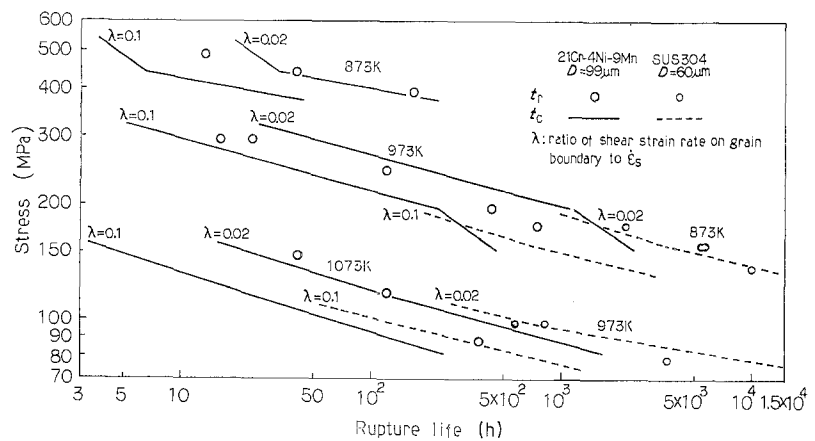


Figure 8 Predicted rupture life,  $t_c$ , and experimental life,  $t_r$ , in austenite steels.

because the effect of the other recovery processes such as plastic relaxation is not taken into account in this model. The model was also applied to the prediction of the rupture life in creep where the wedge-type cracking occurred.

## References

1. J. BRESSERS, "Creep and Fracture in High Temperature Alloys" (Applied Science Publishers, London, 1981) p. 67.
2. R. C. GIFFKINS, *Acta Metall.* **4** (1956) 98.
3. J. E. HARRIS, *Trans. AIME* **233** (1965) 1509.
4. T. MORI, M. KODA, R. MONZEN and T. MURA, *Acta Metall.* **31** (1983) 275.
5. M. TANAKA and H. IIZUKA, *J. Mater. Sci.*, to be published.
6. M. TANAKA, O. MIYAGAWA, T. SAKAKI and D. FUJISHIRO, *Tetsu to Hagane* **65** (1979) 939.
7. J. D. ESHELBY, *Proc. Roy. Soc. A* **241** (1957) 376.
8. T. SAKAKI, *Scripta Metall.* **8** (1974) 189.
9. T. MORI, *Bull. Jpn. Inst. Met.* **17** (1978) 920.
10. W. BEERE and M. V. SPEIGHT, *Met. Sci.* **12** (1978) 593.
11. T. MURA and T. MORI, "Micromechanics" (Baifukan, Tokyo, 1976) p. 105.
12. T. MURA, "Micromechanics of Defects in Solids" (Martinus Nijhoff Publishers, Hague, 1982) p. 74.
13. A. N. STROH, *Proc. Roy. Soc. A* **223** (1954) 404.
14. D. McLEAN, *J. Inst. Met.* **85** (1956-57) 468.
15. F. GAROFALO, translated by M. ADACHI, "Fundamentals of Creep and Creep-Rupture in Metals" Maruzen, Tokyo, 1968) p. 139.
16. H. ABE, "Recrystallization" (Kyoritsu, Tokyo, 1969) p. 162.
17. A. MURAMATSU, *J. Jpn. Soc. Mech. Engrs.* **68** (1965) 1623.
18. S. TAIRA and R. OHTANI, "High-Temperature Strength of Materials" (Ohm, Tokyo, 1980) p. 42.
19. N. SHIN-YA, J. KYONO, H. TANAKA, M. MURATA and S. YOKOI, *Tetsu to Hagane* **69** (1983) 1668.

Received 13 December 1983  
and accepted 2 February 1984